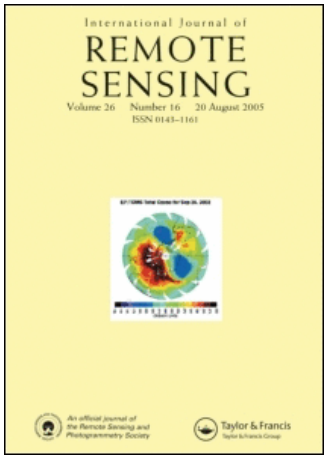

International Journal of Remote Sensing
Publication details, including instructions for authors and subscription information:
http://www.informaworld.com/smpp/title~content=t713722504

Prediction of ocean colour: Monte Carlo simulation applied to a virtual ecosystem based on the Lagrangian Ensemble method

Cheng-Chien Liu [ab]; J. D. Woods [c]
[a] Present address: Department of Earth Sciences, National Cheng Kung University, Tainan, Taiwan 701 ROC
[b] Satellite Geoinformatics Research Centre, National Cheng Kung University, Tainan, Taiwan 701 ROC
[c] Department of Earth Science and Engineering, Imperial College, London SW7 2AZ, UK

Online Publication Date: 01 March 2004
To cite this Article: Liu, Cheng-Chien and Woods, J. D. (2004) 'Prediction of ocean colour: Monte Carlo simulation applied to a virtual ecosystem based on the Lagrangian Ensemble method', International Journal of Remote Sensing, 25:5, 921 - 936
To link to this article: DOI: 10.1080/0143116031000139809
URL: http://dx.doi.org/10.1080/0143116031000139809

INT. J. REMOTE SENSING, 10 MARCH, 2004,
VOL. 25, NO. 5, 921–936

Prediction of ocean colour: Monte Carlo simulation applied to a virtual ecosystem based on the Lagrangian Ensemble method

CHENG-CHIEN LIU†‡ and J. D. WOODS§

†Present address: Department of Earth Sciences, National Cheng Kung University, No. 1, Ta-Hsueh Road, Tainan, Taiwan 701 ROC;
e-mail: ccliu88@mail.ncku.edu.tw
‡Satellite Geoinformatics Research Centre, National Cheng Kung University, No. 1, Ta-Hsueh Road, Tainan, Taiwan 701 ROC
§Department of Earth Science and Engineering, Imperial College, London SW7 2AZ, UK; e-mail: j.woods@ic.ac.uk

(*Received 11 December 2000; in final form 8 April 2003*)

Abstract. The annual variation of ocean-colour signals in the North Atlantic Ocean is successfully simulated by combining the plankton ecosystem model and the optical model. The first model uses the Lagrangian Ensemble method of Woods and Barkmann to simulate the upper-ocean ecosystem, including the vertical profile of chlorophyll concentration. The second model employs the Monte Carlo technique to compute the optical environment for that virtual ecosystem with 31 wavebands in the visible spectrum (400–700 nm). Ocean-colour signals are determined from the spectrum of the relatively few photons that are scattered back up through the sea surface. This information is then substituted into various satellite ocean-colour algorithms to calculate the satellite-derived surface chlorophyll concentration. Results show that substantial differences exist among the predictions from different ocean-colour algorithms. In addition, the average chlorophyll concentration of the upper few layers is not equal to the satellite-derived surface chlorophyll concentration. Our research encourages the adoption of the Monte Carlo optical model to simulate the satellite ocean-colour signals for the purpose of evaluating the plankton ecosystem model.

1. Introduction

Research activities in plankton are intensifying (Mann and Lazier 1996) not only because the ocean contains huge amounts of resources that have direct value to mankind (Summerhayes 1996), but also because plankton plays a major role in the global carbon cycle and therefore the greenhouse effect (Siegenthaler and Sarmiento 1993). Many numerical models have been developed to simulate the plankton ecosystem (Totterdell 1993). However, because of the complicated interaction between individual organisms, populations and environments, it is difficult to validate these models with observations made at sea (Woods 1999).

The significance of deriving near-surface pigment fields from satellite ocean-colour data for initiating and validating numerical models of plankton ecosystems has been emphasized by many international programmes, such as the International Geosphere Biosphere Programme and the Joint Global Ocean Flux Study (Bricaud

International Journal of Remote Sensing
ISSN 0143-1161 print/ISSN 1366-5901 online
http://www.tandf.co.uk/journals
DOI: 10.1080/0143116031000139809

et al. 1999). Satellites provide two-dimensional synoptic viewing, high spatial resolution and low-frequency time series over long periods, even at very isolated ocean locations. Furthermore, area averaging is an automatic result of the remote sensing process. Resulting data are therefore much better suited for applications in the validation of numerical modelling (Robinson 1994). Starting with the mission of the Sea-viewing Wide Field-of-view Sensor (SeaWiFS 1997–present day, there should be nearly continuous ocean-colour measurements for the next 20 years (Abbott *et al.* 1994). In the foreseeable future, high-quality satellite ocean-colour data will be collected multiple times a day (Yoder 1999). This provides a motivation for investigating ways of verifying and correcting the plankton ecosystem models by satellite ocean-colour data.

To evaluate the plankton ecosystem models, the satellite-derived surface chlorophyll-*a* is usually compared with the average chlorophyll concentration of the upper few layers simulated from the plankton ecosystem models. For example, Sarmiento *et al.* (1993) validated their model by comparing the surface chlorophyll concentration map with the Coastal Zone Colour Scanner (CZCS) level 3 monthly composite map. However, at least two possible sources of error are incurred by this approach.

The first source of error is treating the satellite ocean-colour observations as surface quantity. They should be weighted average signals over the first optical attenuation length, and depend on wavelength and the optical properties of the water at that wavelength (Platt and Sathyendranath 1988). Sathyendranath and Platt (1989) pointed out that the satellite-weighted surface concentration *per se* ceases to have ecological significance if the pigment distribution is not uniform. Another source of error is the validation and accuracy of ocean-colour algorithms. Most of the ocean-colour algorithms to date are based on some empirical relationships that are derived from regression analysis on large bio-optical datasets (O'Reilly *et al.* 1998). It has been known for some time that many problems exist for the ocean-colour algorithms (Kahru and Mitchell 1999). A recent example is that after about 300 additional stations were added to the dataset, the OC-2 algorithm had to be revised to maintain a better model–data fit (McClain *et al.* 1998).

In order to avoid such errors in the empirical calibration of ocean-colour algorithm or the assumption of vertical homogeneous distribution, we developed a numerical optical model based on the Monte Carlo ray-tracing technique to simulate the radiative transfer processes both above and below the ocean. In the past two decades, various optical models for solving the radiation transfer equation have been developed (Mobley *et al.* 1993). Recent work by Liu *et al.* (1999, 2002) demonstrates that the numerical optical model was able to provide an accurate simulation of underwater light field. The Monte Carlo method is more direct and comprehensible than other methods, such as the invariant imbedding method or the discrete-ordinates method. Mobley (1994) also pointed out that the Monte Carlo method is competitive with other methods for radiance computations at shallow depths. Therefore, we developed our numerical optical model based on the Monte Carlo method.

Our Monte Carlo model is meticulously validated by careful comparison with a wide range of internal properties of the optical environment with data published by Mobley (1994) for an idealized chlorophyll profile, and against ocean optical measurements. Based on the vertical profiles of chlorophyll in the upper ocean ecosystem simulated by the plankton ecosystem model of Woods and Barkmann (WB) (1994), we were able to simulate the annual variation of the spectrum of

water-leaving radiance in the North Atlantic. This information was then substituted into various ocean-colour algorithms to calculate the ocean-colour signal, i.e. the satellite-derived surface chlorophyll concentration. Results showed that substantial differences existed among the predictions from different ocean-colour algorithms. Additionally, the average chlorophyll concentrations of the upper few layers were not equal to the satellite-derived surface chlorophyll concentration. The simulated spectrum of water-leaving radiance was based on the information of water contents, and it was comparable to the satellite observations. Our research encouraged the adoption of the Monte Carlo optical models to simulate the satellite ocean-colour signals for the purpose of evaluating the plankton ecosystem models.

2. The WB plankton ecosystem model

The WB plankton ecosystem model based on the Lagrangian Ensemble method is a hybrid of the two classical methods for integrating dynamical equations: (1) the Eulerian method, in which the equations are integrated at each location in a fixed grid, and (2) the Lagrangian method, in which the equations are integrated along the trajectory of an object. These equations comprise the physical, chemical and biological processes controlling the ecosystem. All equations and parameters can be found in the paper of Woods and Barkmann (1994) and two technical reports by Barkmann and Woods (1998) and Partridge and Woods (1998).

Each time step in the integration involves four sub-steps: (1) updating the fields of the physical and chemical environment due to external forcing, (2) updating the life histories of each sub-population, (3) computing the new biological fields for each guild from the ensemble statistics of these sub-populations in the physical, chemical and biological fields, and (4) computing the impact of each guild sub-population on the physical, chemical and biological fields.

The WB model possesses two unique features that enable it to simulate the ecosystem more realistically. First, the biological agents used are plankton particles instead of biomass fields. To simulate the life history of every individual plankter is impossible. The WB model allocates each species into a small number of functional guilds and divides each guild population into a manageable set of sub-populations. The life history of each member of the sub-population is identical, while each sub-population behaves like an individual plankter. The simplification and the choice of agents make the WB model a better approach for understanding the complex interaction between individual organisms, population and environment. Second, the ensemble statistics of the population of plankton particles are taken at each time step in the integration to compute food concentration, the impact of predation on prey and the impact of plankton on the environment. This procedure yields fields of biological variables: concentrations of each functional group of plankton stratified by their physiological state. This simplification ensures that we do not need to simulate the interaction of individual predators and prey explicitly. Figure 1 shows the annual distribution of chlorophyll at the Azores (27° W, 41° N), which is one of the simulation results of the WB model. All these chlorophyll profiles, together with meteorological conditions, were fed into our Monte Carlo optical model to simulate the spectrum of water-leaving radiance.

3. The Monte Carlo optical model

The basic principle of the Monte Carlo method is to simulate a beam of light by a very large number of photons. Following the path of each photon, we can use a series of random numbers to determine the photon's life history according

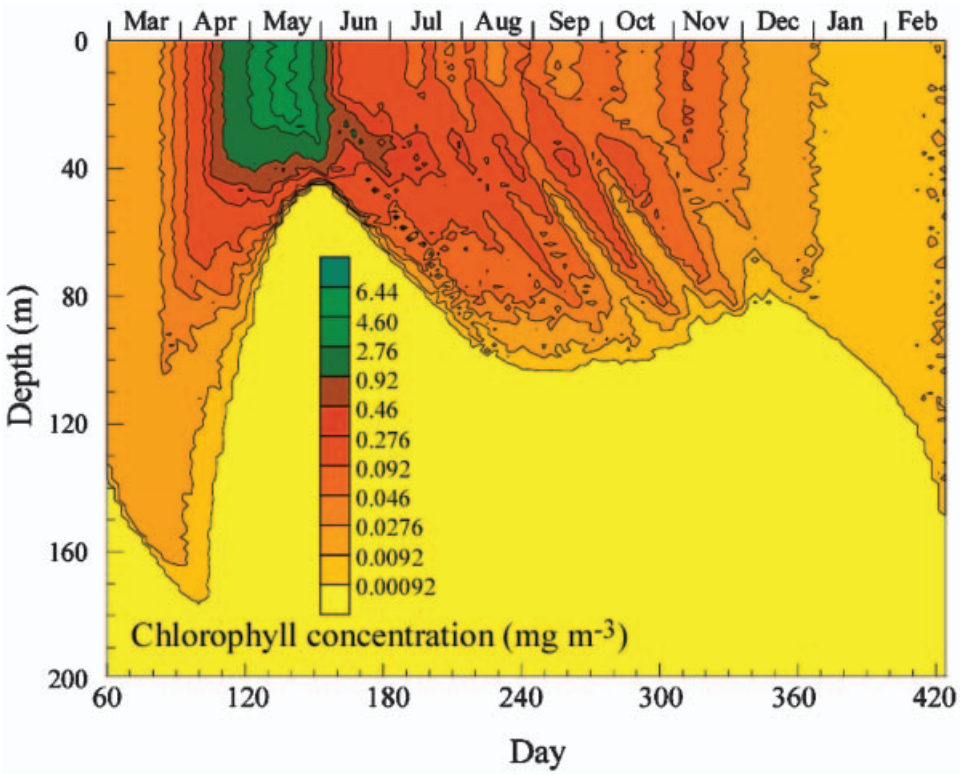

Figure 1. Annual distribution of chlorophyll at the Azores (27° W, 41° N). One of the simulation results of the WB plankton ecosystem model.

to different probabilities for different phenomena. The final light field is the cumulative contribution of total photons.

Our Monte Carlo model is constructed using the basis of models by Kirk (1981) and Tyrrell *et al.* (1999), but improved in two aspects. First, the incident sky radiance at the sea surface is simulated by incorporating a spectral solar irradiance model for cloudless maritime atmospheres (Gregg and Carder 1990), a correction for cloud effect (Kasten and Czeplak 1980), and a model of sky radiance distribution (Harrison and Coombes 1988). Second, the model is enhanced to cope with non-homogeneous water body, i.e. a depth-dependent chlorophyll distribution. Detailed descriptions of all processes are explained as follows.

3.1. *Above the sea surface*

The light from the Sun is a continuous spectrum. It can be discretized into a finite number of wavebands by defining the radiance L at wavelength λ_i as

$$L(\lambda_i) \equiv \frac{1}{\Delta\lambda_i} \int_{\Delta\lambda_i} L(\lambda)\mathrm{d}\lambda \tag{1}$$

In this research, 31 wavebands from 400 to 700 nm are selected with equal $\Delta\lambda_i = 10$ nm.

For a given location, time and date, the incident sky irradiance on the sea surface is calculated from a spectral solar irradiance model for maritime

atmospheres (Gregg and Carder 1990). First, the spectral extraterrestrial solar irradiance $F_o(\lambda)$ is corrected for Earth–Sun orbital distance. It is then attenuated in passing through the atmosphere by Rayleigh scattering, $T_{\text{Rayleigh}}(\lambda)$; ozone, $T_{\text{ozone}}(\lambda)$; oxygen, $T_{\text{oxygen}}(\lambda)$; water vapour absorption, $T_{\text{vapour}}(\lambda)$; marine aerosol after absorption (not scattering), $T_{\text{aerosol, absorption}}(\lambda)$; and marine aerosol, $T_{\text{aerosol, scattering}}(\lambda)$ after scattering (not absorption); and is finally reduced by reflectance at the air–sea interface, R_{dir}. As a result, the clear sky irradiance, $E_{\text{clear}}(\lambda)$; the diffuse sky irradiance, $E_{\text{dif}}(\lambda)$; and the direct sky irradiance $E_{\text{dir}}(\lambda)$ can be expressed as

$$\begin{aligned}
&E_{\text{clear}}(\lambda) = E_{\text{dir}}(\lambda) + E_{\text{dif}}(\lambda),\\
&E_{\text{dir}}(\lambda) = F_o(\lambda)\cos\theta_s T_{\text{Rayleigh}} T_{\text{ozone}} T_{\text{aerosol, absorption}} T_{\text{oxygen}} T_{\text{vapour}}(1-R_{\text{dir}}),\\
&E_{\text{dif}}(\lambda) = F_o(\lambda)\cos\theta_s T_{\text{ozone}} T_{\text{oxygen}} T_{\text{vapour}}(1-R_{\text{dir}})\\
&\left[0.5 T_{\text{aerosol, absorption}}\left(1 - T_{\text{Rayleigh}}^{0.95}\right) + T_{\text{Rayleigh}}^{1.5} T_{\text{aerosol, absorption}} F_a\left(1 - T_{\text{aerosol, scattering}}\right)\right]
\end{aligned} \tag{2}$$

where θ_s is the solar zenith angle, and F_a is the forward scattering probability of the aerosol. A detailed description of the equations and variables can be found in Gregg and Carder (1990). Note that this simple spectral sky irradiance model is specific for oceanographic applications for clear sky. If cloud cover is higher than 25%, a correction (Kasten and Czeplak 1980) is applied to calculate the cloudy sky irradiance:

$$\begin{aligned}
E_{\text{cloudy}}(\lambda) &= E_{\text{clear}}(\lambda)\left(1 - 0.75 Cloud^{3.4}\right),\\
E_{\text{dif}}(\lambda) &= E_{\text{cloudy}}(\lambda)\left(0.3 + 0.7 Cloud^2\right),\\
E_{\text{dir}}(\lambda) &= E_{\text{cloudy}}(\lambda) - E_{\text{dif}}(\lambda)
\end{aligned} \tag{3}$$

where *Cloud* is the cloud cover (in tenths).

The sky irradiance, as well as the radiance distribution, is required to trace the actual directions of incident photons. Harrison and Coombes (1988) analysed the radiometer data collected between July 1983 and March 1986 at a rural site in the Rocky Mountain foothills. The results showed that the normalized sky radiance $N(\theta, \phi)$ can be given analytically by combining the normalized overcast sky radiance $N_o(\theta, \phi)$ and the normalized clear sky radiance $N_c(\theta, \phi)$:

$$\begin{aligned}
&N(\theta, \phi) = Cloud N_O(\theta, \phi) + (1 - Cloud) N_c(\theta, \phi),\\
&N_o(\theta, \phi) = 0.45 + 0.12\theta_s + 0.43\cos\theta + 0.72 e^{-1.88\psi},\\
&N_c(\theta, \phi) = \left(1 - e^{-0.19\sec\theta}\right)\left(1 - e^{-0.53\sec\theta_s}\right)\left(1.63 + 53.7 e^{-5.49\psi} + 2.04\cos^2\psi\cos\theta_s\right)
\end{aligned} \tag{4}$$

where θ is the sky zenith angle, ϕ is the sky azimuth angle relative to the Sun, θ_s is the solar zenith angle, and ψ is the scattering angle between sky and the Sun directions. The model of Harrison and Coombes (1988) is employed to determine the incident direction of each photon.

3.2. *On the sea surface*

The sea surface is usually roughened by wind. The relation between the mean-square wave slope σ^2 over the sea surface and the surface wind speed V_{wind} can be described by an equation proposed by Cox and Munk (1954):

$$\sigma^2 = 0.003 + 0.00512 V_{\text{wind}}. \tag{5}$$

Sathe and Sathyendranath (1992) pointed out that by assuming further the distribution of wave slopes around their mean to be Gaussian (Preisendorfer 1976),

the probability function $P(\phi_{ws})$ of the occurrence of wave slope can be expressed as

$$P(\phi_{ws}) = \exp\left(\frac{-\tan^2\phi_{ws}}{2\sigma^2}\right) \tag{6}$$

where ϕ_{ws} is the angle between the vertical and the normal to the sea surface at a given point.

When photons arrive at the sea surface, some will reflect up, while some will penetrate into the sea. Their trajectories follow the general geometric optical rules:

$$\begin{aligned}
\mathbf{r} &= \mathbf{p} - 2(\mathbf{p}\cdot\mathbf{n})\mathbf{n}, \\
\mathbf{t_a} &= \frac{1}{n_w}\left\{\mathbf{p} - \left[\mathbf{p}\cdot\mathbf{n} + \sqrt{(\mathbf{p}\cdot\mathbf{n})^2 + n_w^2 - 1}\right]\mathbf{n}\right\}, \\
\mathbf{t_w} &= n_w\mathbf{p} - \left[n_w\mathbf{p}\cdot\mathbf{n} - \sqrt{(n_w\mathbf{p}\cdot\mathbf{n})^2 - n_w^2 + 1}\right]\mathbf{n}
\end{aligned} \tag{7}$$

This equation describes the relationship between the incident ray **p**, the reflected ray **r**, and the transmitted ray $\mathbf{t_a}$, $\mathbf{t_w}$ (subscripts a and w stand for the air-incident and water-incident cases, respectively). **n** is a unit vector normal to the surface and is directed upward. n_w is the index of refraction for water.

The reflectance $r(\theta_p)$ for either the air-incident or the water-incident case is given by Fresnel's formula (Sears 1948):

$$\begin{aligned}
r(\theta_p \neq 0) &\equiv \frac{1}{2}\left\{\left[\frac{\sin(\theta_p - \theta_t)}{\sin(\theta_p + \theta_t)}\right]^2 + \left[\frac{\tan(\theta_p - \theta_t)}{\tan(\theta_p + \theta_t)}\right]^2\right\}, \\
r(\theta_p = 0) &\equiv \left(\frac{n_w - 1}{n_w + 1}\right)^2,
\end{aligned} \tag{8}$$

where θ_p is the incident angle between **p** and **n**, and θ_t is the transmitted angle between **t** and **n**. This probability can be further corrected by taking the white cap effect into consideration (Kirk 1994), which results in

$$\Delta r(\theta_p) = 0.22 \times 2.692 \times 10^{-5} \times V_{wind}^{2.625} \tag{9}$$

3.3. *Below the sea surface*

Once a photon enters the seawater, a series of complicated phenomena will occur. The path length ℓ of a photon before it hits another particle is given by the equation (Gordon 1994):

$$\ell = \frac{-1}{c(z, \lambda)}\ln(\rho_j) \tag{10}$$

The beam attenuation coefficient $c(z, \lambda)$ is a function of depth z and wavelength λ in non-homogeneous water. ρ_j is a sequence of random numbers between 0 and 1. Once the collision occurs, the photon will be either absorbed or scattered. Its fate can be determined by the inherent optical properties (IOPs) at that particular depth, provided the profiles of the IOPs are measured. If only the profile of chlorophyll is available, two bio-optical algorithms that relate the local content of chlorophyll concentration to the absorption and scattering coefficients should be employed.

The spectral absorption coefficient $a(\lambda)$ of case 1 waters is obtained using the

models of Morel (1991) and Prieur and Sathyendranath (1981):

$$a(z;\lambda)=\left[a_{\mathrm{w}}(\lambda)+0.06a_{\mathrm{c}}^{*}(\lambda)C(z)^{0.65}\right]\left[1+a_{\mathrm{other}}\exp(-0.014(\lambda-440))\right] \qquad (11)$$

where $a_{\mathrm{w}}(\lambda)$ is the absorption coefficient of pure water taken from Smith and Baker (1981), and C is the chlorophyll-*a* concentration ($\mathrm{mg\,m^{-3}}$). $a_{\mathrm{c}}^{*}(\lambda)$ is the normalized chlorophyll-specific absorption coefficient (Morel 1988) and is equal to one at a reference wavelength 440 nm (i.e. $a_{\mathrm{c}}^{*}(440)=1$). This model assumes that a fixed percentage of the total absorption at a given wavelength always comes from yellow matter, and $a_{\mathrm{other}}\equiv a_{\mathrm{g}}=0.2$. The scattering coefficient $b(\lambda)$ is derived from the model of Gordon *et al.* (1983) and Morel (1991):

$$b(z;\lambda)=0.3\left(\frac{550}{\lambda}\right)C(z)^{0.62}+b_{\mathrm{w}}(\lambda) \qquad (12)$$

where $b_{\mathrm{w}}(\lambda)$ is the spectral scattering coefficient of pure water as taken from Smith and Baker (1981).

The absorption and scattering coefficients are used to determine whether this particular photon is absorbed or scattered. If absorbed, current ray tracing is finished and another photon is submitted. If scattered, the normalized volume-scattering phase function (VSF)

$$\tilde{\beta}(\psi;\lambda)\equiv\frac{b_{\mathrm{w}}(\lambda)}{b(\lambda)}\tilde{\beta}_{\mathrm{w}}(\psi)+\frac{b_{\mathrm{p}}(\lambda)}{b(\lambda)}\tilde{\beta}_{\mathrm{p}}(\psi;\lambda) \qquad (13)$$

is used to determine the scattering angle. ψ is the scattering angle and $b_{\mathrm{p}}(\lambda)$ is the spectral scattering coefficient of particles. $\tilde{\beta}_{\mathrm{w}}$ and $\tilde{\beta}_{\mathrm{p}}$ are normalized VSFs contributed from water and particle, respectively. Mobley (1994) derived $\tilde{\beta}_{\mathrm{p}}$ from three sets of Petzold's data (Petzold 1977) as follows: (1) subtract $\beta_{\mathrm{w}}(\psi;\ \lambda=514\,\mathrm{nm})$ from each curve to get three particle VSFs $\beta_{\mathrm{p}}^{i}(\psi)$, $i=1, 2, 3$; (2) obtain the corresponding particle-scattering coefficients from $b_{\mathrm{p}}^{i}=b^{i}-b_{\mathrm{w}}$; (3) compute $\tilde{\beta}_{\mathrm{p}}^{i}(\psi)=\beta_{\mathrm{p}}^{i}(\psi)\Big/b_{\mathrm{p}}^{i}$; and (4) average the three particle VSFs at each scattering angle to define $\tilde{\beta}_{\mathrm{p}}(\psi)$. These results are listed in table 3.10 in Mobley (1994). With this table, the normalized VSF can be specified.

Most photons will be absorbed in the water. Only a small fraction of photons is scattered back to the sky. The final light field is obtained by registering the cumulative contribution of total photons at each depth. The source code of this Monte Carlo optical model is available by request from the authors.

4. Validation

Validation of the Monte Carlo optical model is crucial before further simulation of the signal of ocean colour and light field. However, due to the lack of comprehensive simultaneous measurements of IOPs, environment parameters and radiometric distribution, it is not presently possible to make a straightforward model–data comparison. Mobley (1994) has made a series of 'case studies' based on another numerical model: the invariant imbedding method. By 'turning on and off' physical processes, he was able to gain insight into the importance of each process in nature and built up a reliable optical model step by step. We followed the same procedure to validate our Monte Carlo model.

Figure 2 shows the results of the model-to-model comparison. All the figures are plotted using the same scale as the figures in Mobley (1994) (figures 11.1, 11.3 and 11.6). The radiance L is plotted as a function of the viewing direction $(\theta_{\mathrm{v}}, \phi_{\mathrm{v}})$ in the plane of the sun. Figure 2(*a*) is simulated at three selected optical depths ($\zeta=0$, 5 and

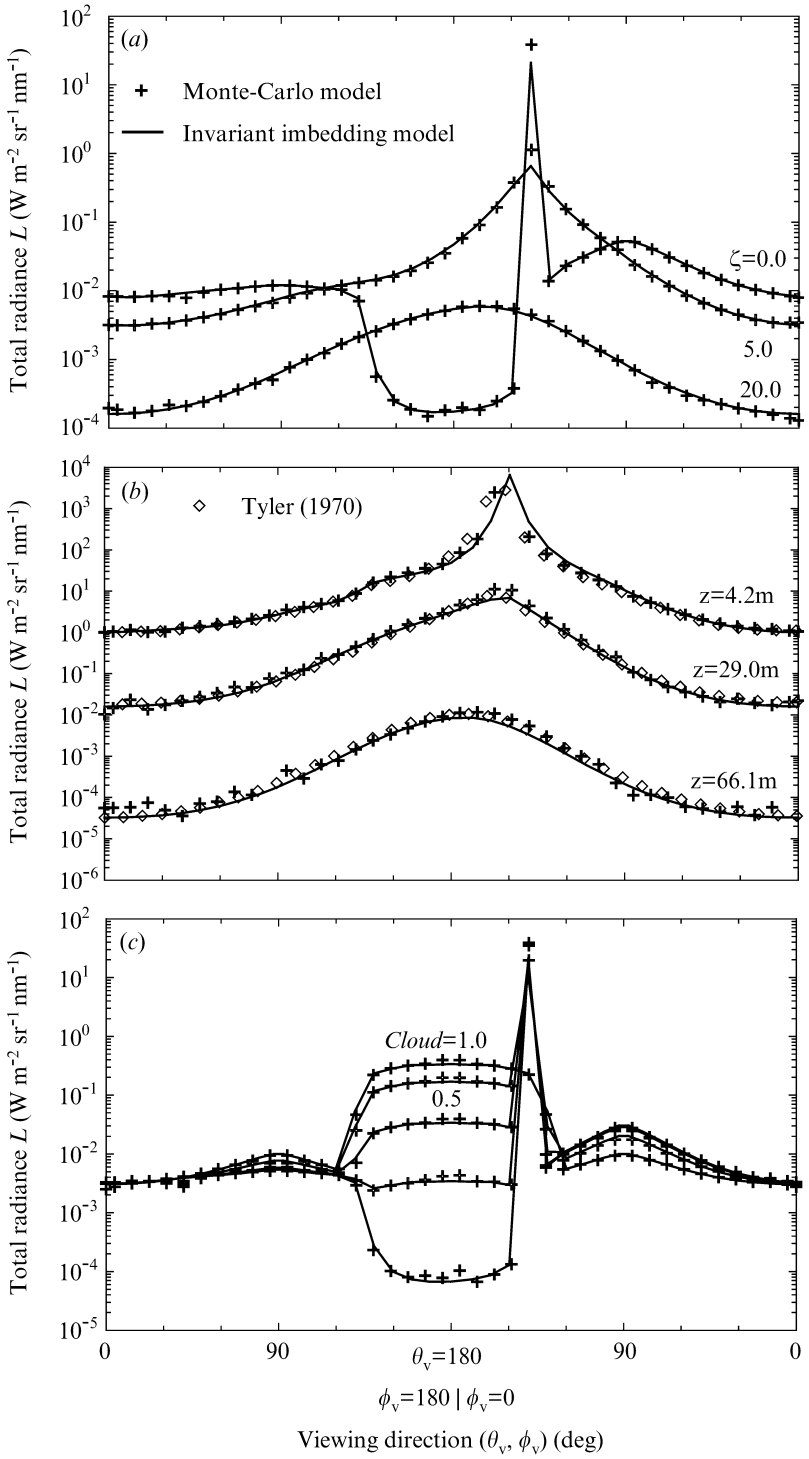

Figure 2. Model validation: comparison of the Monte Carlo model and the invariant imbedding model. This is a direct comparison with figures 11.1, 11.3 and 11.6 in Mobley (1994).

20) in the most simplified conditions: the sea water is homogeneous with high albedo $\omega_0 = 0.9$; the scattering phase function is taken as the average particle VSF; the sea surface is level; there is only one unit of solar irradiance, at zenith angle $\theta_s = 60^\circ$; and the sky is black. Figure 2(*b*) simulates the data of Tyler and Smith (1970) under the above conditions with the following modifications: $\omega_0 = 0.7$; there is one unit of solar irradiance at zenith angle $\theta_s = 38^\circ$ and the sky irradiance is distributed by $E = 0.1 \times E_{sky} + 0.9 \times E_{Sun}$, where E_{sky} is the background diffuse irradiance with a uniform distribution. The sky radiance effect under different cloud-cover conditions is shown in figure 2(*c*). The simulated conditions are as follows: $\omega_0 = 0.8$; there is one unit of solar irradiance at zenith angle $\theta_s = 57^\circ$ and the sky irradiance is distributed by $E = Cloud \times E_{sky} + (1 - Cloud) \times E_{Sun}$, where E_{sky} is taken to be cardioidal distribution $L(\theta, \phi) = L_0(1 + 2\cos\theta)$. The remarkable consistency seen in figure 2 confirms that the various physical processes simulated in our model are accurate. The very small discrepancies result from the different directional discretizations used in these models.

5. Results and discussion

5.1. *Maximum and minimum production days at the Azores*

The Azores (27° W, 41° N) is a place where the heat received and lost within 1 year is balanced. In addition, the slowed ocean current near the islands provides a water column similar to that used in the WB model. This model has been applied to simulate the plankton ecosystem at the Azores (Woods and Barkmann 1994). We chose the maximum and minimum primary production days during 1 year, 13 May and 17 January, respectively (see figure 1). Figure 3(*a*) presents the chlorophyll

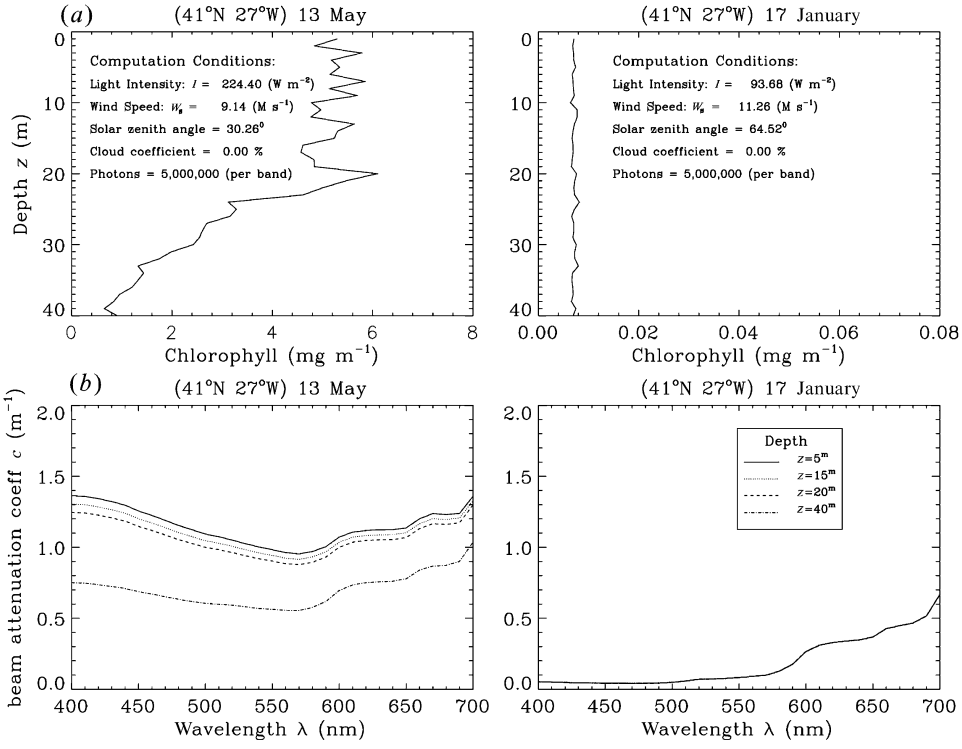

Figure 3. The chlorophyll profiles and the beam attenuation coefficient $c(z,\lambda)$ on the maximum and minimum production days at the Azores.

profile and meteorological conditions at midday. These data are fed into our Monte Carlo model to simulate the light field, which is then integrated on an SGI Challenge computer. It takes about 6 h to simulate 1 year of change in the virtual ecosystem and 250 s per million photons per waveband to calculate the light field.

There are two orders of variation in the chlorophyll in the upper 40 m, between the maximum and minimum production days; the chlorophyll concentration profoundly influences the IOPs of seawater and causes the light field to change dramatically. The depth-dependent chlorophyll concentrations $C(z)$ are substituted into equations (11)–(13) to calculate the IOPs. Figure 3(*b*) gives the beam attenuation coefficient $c(z, \lambda)$ at selected depths and wavelengths. Chlorophyll dominates both the absorption and scattering characteristics of plankton-rich water, especially in the blue wavebands. Water itself is responsible for attenuation in the plankton-poor environment and influences both the red and green wavebands. The unequally distributed spectra reflected upward and penetrating downward are generated as a result.

Figure 4 shows the simulated apparent optical properties on the maximum and minimum production days of the Azores. Figure 4(*a*) and (*b*) are the spectral downward and upward planar irradiances at selected depths. It is generally accepted that pure seawater is deep blue while plankton-rich water is murky green. Figure 4(*a*) and (*b*) illustrate this phenomenon. The chlorophyll absorbs blue light, but reflects red and green. Water, on the other hand, absorbs most of the red and some of the green light, but reflects blue. The deeper the water, the more obvious this phenomenon. The colour below the surface is very different from the colour observed at the surface.

The zenith radiance $L_u(z, \lambda)$ and the water-leaving radiance $L_w(\lambda)$ are plotted in figure 4(*c*). L_u is the radiance heading straight upward, i.e. $\theta = \pi$. $z = 0^+$ and 0^- represent the radiance just above and just below the sea surface, respectively. L_w is the upwelling radiance measured in the air just above the water surface. It should be noted that $L_u(0^+)$ includes both emergent flux as well as surface-reflected light, whereas L_w represents only the emergent flux. For the applications in satellite ocean-colour observations, the atmospheric influences are removed from the total radiative signals to retrieve L_w. Our Monte Carlo optical model separates the emergent flux from the surface-reflected light. Therefore, L_w can be simulated and compared with the satellite sensor data directly.

5.2. *Simulations of ocean-colour signal off the Azores*

The satellite ocean-colour signal is calculated from relative amounts of L_w in selected wavebands in the visible spectrum. This signal is usually correlated to the surface chlorophyll concentration by an empirical ocean-colour algorithm. Our research applies the Monte Carlo optical model to simulate the spectral signal of L_w directly, rather than treating the ocean-colour signal as the surface chlorophyll concentration and comparing this signal to the averaged value taken from the output of the WB model in the upper few metres.

The procedure for running the Monte Carlo model is briefly described as follows: first, the WB model is initialized by running at the Azores for 5 years until all components in the model simulation stabilized. The same model is continued for another year, beginning on the first of March. Every 10 days, the chlorophyll profiles along with the meteorological conditions are fed into

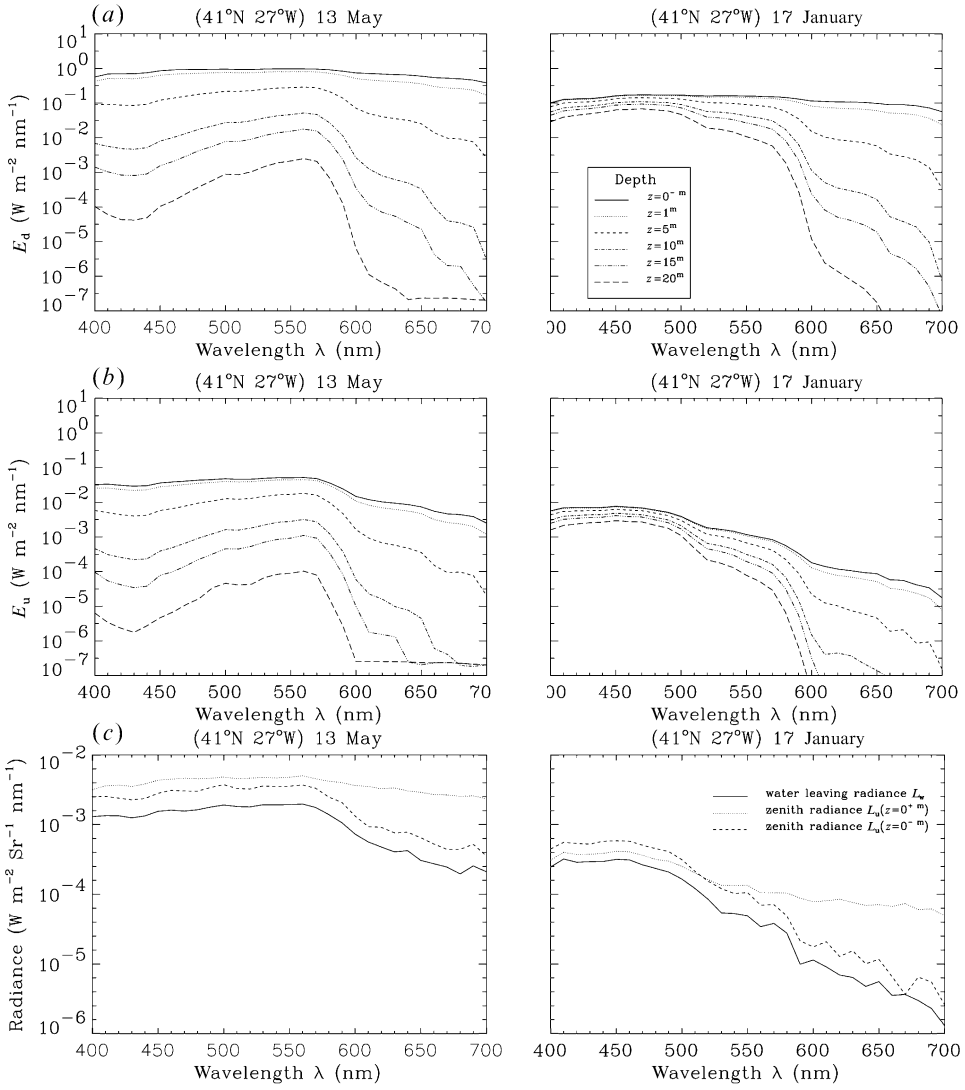

Figure 4. The apparent optical properties on the maximum and minimum production days at the Azores.

our Monte Carlo optical model. The spectral information of L_w at the CZCS and the SeaWiFS wavelengths (443, 490, 520, 550 and 555 nm; bandwidths of 20 nm) is simulated directly. The satellite-derived chlorophyll concentration C_{sd} (mg m^{-3}) is then calculated from $L_w(\lambda)$ using the CZCS algorithm (Gordon *et al.* 1983):

$$\begin{cases} C_{sd} = 1.130\left(\dfrac{L_{w,\,443}}{L_{w,\,550}}\right)^{-1.710} & \text{for } C_{sd} < 1.5 \\ C_{sd} = 3.326\left(\dfrac{L_{w,\,520}}{L_{w,\,550}}\right)^{-2.439} & \text{for } C_{sd} > 1.5 \end{cases} \tag{14}$$

the SeaWiFS OC2-v1 algorithm (O'Reilly *et al.* 1998):

$$C_{sd} = -0.04 + 10^{(0.341 - 3.001X + 2.811X^2 - 2.041X^3)} \tag{15}$$

the SeaWiFS OC2-v2 algorithm (McClain *et al.* 1998):

$$C_{sd} = -0.0929 + 10^{(0.2974 - 2.2429X + 0.8358X^2 - 0.0077X^3)} \tag{16}$$

and the latest SeaWiFS OC2-v4 algorithm (O'Reilly *et al.* 2000):

$$C_{sd} = -0.071 + 10^{(0.319 - 2.336X + 0.879X^2 - 0.135X^3)} \tag{17}$$

to simulate the satellite-derived pigment concentration, where X is the log value of the ratio of remote sensing reflectance at band 490 and 555 nm.

Figure 5(*a*) displays the simulated $L_w(\lambda)$ at five wavelengths. In general, the intensity of $L_w(\lambda)$ is influenced mainly by the magnitude of solar flux, which increases in the spring, peaks in midsummer, and decreases in the winter. The

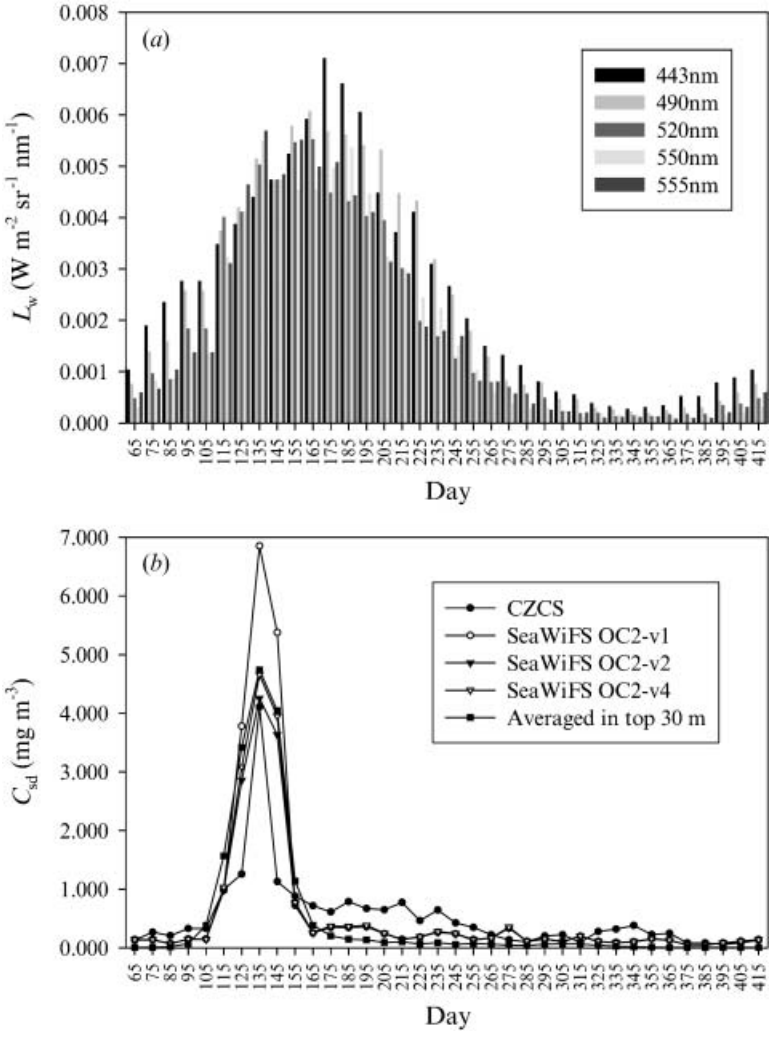

Figure 5. Simulations of the time series of satellite-derived chlorophyll concentration C_{sd} (mg m^{-3}) off the Azores based on the various ocean-colour algorithms (equations (14)–(17)).

spectral ratio of $L_w(\lambda)$, however, is influenced by the variation of oceanic contents, mainly the phytoplankton. The purpose of satellite ocean-colour observation is to infer the water contents from these slight differences in the ratio of spectral signals. Based on the CZCS and SeaWiFS OC2 ocean-colour algorithms (equations (14)–(17)), the corresponding time series of C_{sd} off the Azores are given in figure 5(*b*). The averaged values of chlorophyll concentration in the upper 30 m taken from the WB model are also plotted in the same figure for comparison. Remarkably, all satellite-derived chlorophyll concentrations give comparable values, to first order, in spite of the different algorithms employed. Substantial deviations are apparent, however, among the predictions from various algorithms during the spring bloom. Compared to the depth-averaged values taken from the WB model, the performance of the SeaWiFS OC2 algorithms is better than the earlier CZCS algorithm, and the latest version OC2-v4 is much improved over the previous versions OC2-v2 and OC2-v1. However, as previously mentioned, the satellite ocean-colour observation is a weighted average signal over the first optical attenuation length, which depends on wavelengths and on the optical properties of the water at each wavelength. It is not unreasonable to expect deviations between these averaged values and the satellite-derived concentrations. This research suggests that for the purposes of validating a plankton ecosystem model with satellite ocean-colour observations, it is necessary to apply an Monte Carlo optical model to simulate the emergent light field when comparing this information with satellite-derived chlorophyll concentrations.

To investigate the WB model geographically and temporally, we extended our simulation to the North Atlantic Ocean from 20° N to 50° N along 20° W. Figure 6 shows the simulated results of ocean-colour signals from 20° N to 50° N along 20° W using SeaWiFS OC2-v4 algorithm. As one moves northward in the North Atlantic Ocean, the spring bloom occurs later in the year and with greater intensity (Mann and Lazier 1996). The WB model gives a reasonable simulation of the poleward migration of the spring bloom that matches these observations well.

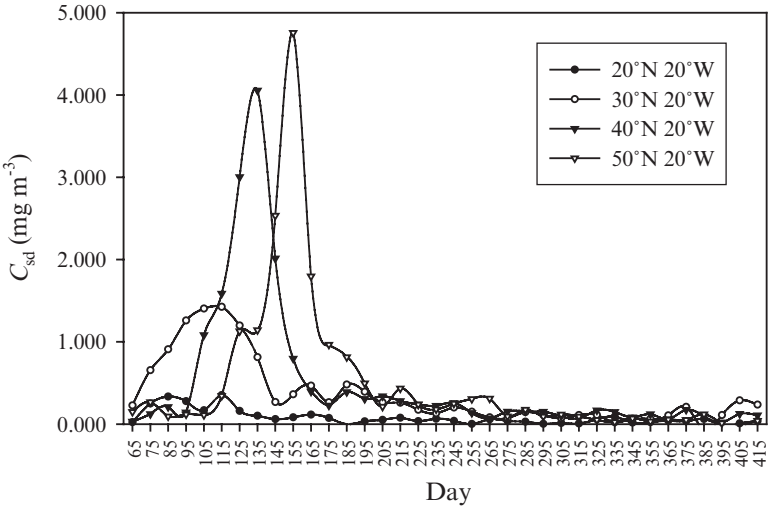

Figure 6. Simulations of the time series of satellite-derived chlorophyll concentration C_{sd} (mg m^{-3}) using SeaWiFS OC2-v4 algorithm in the North Atlantic Ocean from 20° N to 50° N along 20° W.

Results from this research have been applied to quantitatively test the WB plankton ecosystem model by means of SeaWiFS ocean-colour observations (Liu 2000). This involves a new approach of retrieving information from patchy observations of ocean colour (Liu and Woods, submitted).

6. Summary

A Monte Carlo optical model has been constructed. This model has been validated through careful comparison with a wide range of IOPs found in the natural environment with data published by Mobley (1994) for an idealized chlorophyll profile and against ocean optical measurements. The WB plankton ecosystem model is used to simulate the plankton ecosystem in the North Atlantic Ocean. These spatial and temporal results, along with the meteorological conditions, are fed into the Monte Carlo optical model to simulate the annual variation of the emergent light field. This information is then substituted into various satellite ocean-colour algorithms to calculate C_{sd}. Results clearly show substantial differences among the predictions from different ocean-colour algorithms. In addition, the average chlorophyll concentrations of the upper few layers are not equal to C_{sd}. Our research encourages the adoption of the Monte Carlo optical model to simulate the satellite ocean-colour signals for the purpose of evaluating the plankton ecosystem models.

Acknowledgments

We thank Dr Toby Tyrrell for his help in the beginning stage of constructing the Monte Carlo optical model. This research was supported by the UK Natural Environment Research Council SOC, an Overseas Research Student (ORS) award from the UK committee of vice-chancellors and principals (CVCP), and a research studentship from the Ministry of Education, Taiwan Republic of China. Part of this work was performed while C.-C. Liu held a National Research Council Research Associateship at NASA John C. Stennis Space Center. This work was also supported by the National Science Council of Taiwan (NSC 92-2611-M-006-002).

References

ABBOTT, M. R., BROWN, O. B., GORDON, H. R., CARDER, K. L., EVANS, R. E., MULLER-KARGER F. E., and ESAIAS, W. E., 1994, Ocean color in the 21st century: a strategy for a 20-year time series. NASA Technical Memorandum 104566, NASA Goddard Space Flight Center, Greenbelt, Maryland, USA.

BARKMANN, W., and WOODS, J., 1998, The Lagrangian Ensemble model LE'98 science modules, 6. Imperial College of Science, Technology and Medicine, London.

BRICAUD, A., MOREL, A., and BARALE, V., 1999, MERIS potential for ocean colour studies in the open ocean. *International Journal of Remote Sensing*, **20**, 1757–1769.

COX, C., and MUNK, W., 1954, The measurement of the roughness of the sea surface from photographs of the sun's glitter. *Journal of the Optical Society of America*, **44**, 838–850.

GORDON, H. R., 1994, Modeling and simulating radiative transfer in the ocean. In *Ocean Optics*, edited by R. W. Spinrad, K. L. Carder and M. J. Perry (New York: Oxford University Press), pp. 3–39.

GORDON, H. R., CLARK, D. K., BROWN, J. W., BROWN, O. B., EVANS, R. H., and BROENKOW, W. W., 1983, Phytoplankton pigment concentrations in the Middle Atlantic Bight: comparison of ship determinations and CZCS estimates. *Applied Optics*, **22**, 20–36.

GREGG, W. W., and CARDER, K. L., 1990, A simple spectral solar irradiance model for cloudless maritime atmospheres. *Limnology and Oceanography*, **35**, 1657–1675.

HARRISON, A. W., and COOMBES, C. A., 1988, An opaque cloud cover model of sky short wavelength radiance. *Solar Energy*, **41**, 387–392.

KAHRU, M., and MITCHELL, B. G., 1999, Empirical chlorophyll algorithm and preliminary SeaWiFS validation for the California Current. *International Journal of Remote Sensing*, **20**, 3423–3429.

KASTEN, F., and CZEPLAK, G., 1980, Solar and terrestrial radiation dependent on the amount and type of cloud. *Solar Energy*, **24**, 177–189.

KIRK, J. T. O., 1981, Monte Carlo procedure for simulating the penetration of light into natural waters. CSIRO Australia Division of Plant Industry Technical Paper, 36, 1–16.

KIRK, J. T. O., 1994, *Light and Photosynthesis in Aquatic Ecosystems*, 2nd edn (Cambridge: Cambridge University Press).

LIU, C.-C., 2000, Using SeaWiFS ocean colour data to test a plankton ecosystem model. PhD thesis, Imperial College, University of London.

LIU, C.-C., and WOODS, J., 2003, Retrieving information from patchy observations of ocean color for validating a plankton ecosystem model. *Deep-Sea Research II* (accepted).

LIU, C.-C., WOODS, J. D., and MOBLEY, C. D., 1999, Optical model for use in oceanic ecosystem models. *Applied Optics*, **38**, 4475–4485.

LIU, C.-C., CARDER, K. L., MILLER, R. L., and IVEY, J. E., 2002, Fast and accurate model of underwater scalar irradiance. *Applied Optics*, **41**, 4962–4974.

MANN, K. H., and LAZIER, J. R. N., 1996, *Dynamics of Marine Ecosystems*, 2nd edn (Oxford: Blackwell).

MCCLAIN, C. R., CLEAVE, M. L., FELDMAN, G. C., GREGG, W. W., HOOKER, S. B., and KURING, N., 1998, Science quality SeaWiFS data for global biosphere research. *Sea Technology*, **39**, 10–16.

MOBLEY, C. D., 1994, *Light and Water: Radiative Transfer in Natural Waters* (San Diego, CA: Academic Press).

MOBLEY, C. D., GENTILI, B., GORDON, H. R., JIN, Z., KATTAWAR, G. W., MOREL, A., REINERSMAN, P., STAMNES, K., and STAVN, R. H., 1993, Comparison of numerical models for computing underwater light fields. *Applied Optics*, **32**, 7484–7504.

MOREL, A., 1988, Optical modelling of the upper ocean in relation to its biogenous matter content (case 1 water). *Journal of Geophysical Research*, **93**, 10749–10768.

MOREL, A., 1991, Light and marine photosynthesis: a spectral model with geochemical and climatological implications. *Progress in Oceanography*, **26**, 263–306.

O'REILLY, J. E., MARITORENA, S., MITCHELL, B. G., SIEGEL, D. A., CARDER, K. L., GARVER, S. A., KAHRU, M., and MCCLAIN, C., 1998, Ocean color chlorophyll algorithms for SeaWiFS. *Journal of Geophysical Research*, **103**, 24937–24953.

O'REILLY, J. E., MARITORENA, S., O'BRIEN, M. C., SIEGEL, D. A., TOOLE, D., MENZIES, D., SMITH, R. C., MUELLER, J. L., MITCHELL, B. G., KAHRU, M., CHAVEZ, F. P., STRUTTON, P. G., COTA, G. F., HOOKER, S. B., MCCLAIN, C. R., CARDER, K. L., MULLER-KARGER, F., HARDING, L., MAGNUSON, A., PHINNEY, D., MOORE, G. F., AIKEN, J., ARRIGO, K. R., LETELIER, R. M., and CULVER, M., 2000, SeaWiFS postlaunch calibration and validation analyses, part 3. NASA Technical Memorandum 2000-206892, NASA Goddard Space Flight Center, Greenbelt, Maryland, USA.

PARTRIDGE, L., and WOODS, J., 1998, The ZB model, 4. Imperial College of Science, Technology and Medicine, London.

PETZOLD, T. J., 1977, Volume scattering functions for selected ocean waters. In *Light in the Sea*, edited by J. E. Tyler (Stroudsberg: Dowden, Hutchinson and Ross), pp. 152–174.

PLATT, T., and SATHYENDRANATH, S., 1988, Oceanic primary production: estimation by remote sensing at local and regional scales. *Science*, **241**, 1613–1620.

PREISENDORFER, R. W., 1976, *Hydrologic Optics* (Seattle, WA: U.S. Department of Commerce).

PRIEUR, L., and SATHYENDRANATH, S., 1981, An optical classification of coastal and oceanic waters based on the specific spectral absorption curves of phytoplankton pigments, dissolved organic matter, and other particulate materials. *Limnology and Oceanography*, **26**, 671–689.

ROBINSON, I. S., 1994, *Satellite Oceanography: an Introduction for Oceanographers and Remote-sensing Scientists*, 2nd edn (Chichester: John Wiley & Sons).

SARMIENTO, J. L., SLATER, R. D., FASHAM, M. J. R., DUCKLOW, H. W., TOGGWEILER, J. R., and EVANS, G. T., 1993, A seasonal three-dimensional ecosystem model of nitrogen cycling in the North Atlantic euphotic zone. *Global Biogeochemical Cycles*, **7**, 417–450.

SATHE, P. V., and SATHYENDRANATH, S., 1992, A Fortran-77 program for Monte Carlo simulation of upwelling light from the sea. *Computers and Geosciences*, **18**, 487–507.

SATHYENDRANATH, S., and PLATT, T., 1989, Remote sensing of ocean chlorophyll: consequences of nonuniform pigment profile. *Applied Optics*, **28**, 490–495.

SEARS, F. W., 1948, *Principles of Physics: 3. Optics* (Cambridge, MA: Addison-Wesley).

SIEGENTHALER, U., and SARMIENTO, J. L., 1993, Atmospheric carbon dioxide and the ocean. *Nature*, **365**, 119–125.

SMITH, R. C., and BAKER, K., 1981, Optical properties of the clearest natural waters. *Applied Optics*, **20**, 177–184.

SUMMERHAYES, C. P., 1996, Ocean resources. In *Oceanography: an Illustrated Guide*, edited by C. P. Summerhayes and S. A. Thorpe (London: Manson), pp. 314–337.

TOTTERDELL, I. J., 1993, An annotated bibliography of marine biological models. In *towards a Model of Biogeochemical Processes*, edited by G. T. Evans and M. J. R. Fasham (Berlin: Springer-Verlag), pp. 317–339.

TYLER, J. E., and SMITH, R. C., 1970, *Measurements of Spectral Irradiance Underwater* (New York: Gordon and Breach).

TYRRELL, T., HOLLIGAN, P. M., and MOBLEY, C. D., 1999, Optical impacts of oceanic coccolithophore blooms. *Journal of Geophysical Research*, **104**, 3223–3241.

WOODS, J. D., 1999, Understanding the ecology of plankton. *Academia Europaea*, **7**, 371–384.

WOODS, J. D., and BARKMANN, W., 1994, Simulating plankton ecosystems by the Lagrangian Ensemble method. *Philosophical Transactions of the Royal Society*, B, **343**, 27–31.

YODER, J. A., 1999, Status and plans for satellite ocean-colour missions: considerations for complementary missions. IOCCG Report 2, Dartmouth, Canada.